

## Synthesis, characterization and hydrophilic properties of nanocrystalline $ZnCo_2O_4$ oxide by combustion route

Sachin. V. Bangale, S. M. Khetre and S. R. Bamane\*

Metal Oxide Research Laboratory, Department of Chemistry, Dr. Patangrao Kadam Mahavidyalaya, Sangli (M.S.) India

---

### ABSTRACT

The aim of said study was to obtain nanostructured  $ZnCo_2O_4$  through self combustion synthesis using cobalt nitrate, iron nitrate as precursors and glycine as a fuel, without the subsequent heat treatments after synthesis. The temperature variation with respect to a sample with constant molar ratio was investigated. The crystallinity (phases present and crystallite size: estimated by single-line method) of the product obtained was determined by X-ray diffraction (XRD) measurement, thermogravimetric analysis(TG-DTA),scanning electron microscope(SEM),and high resolution transmission electron microscopy (HRTEM). The synthesis method facilitated the production of spinel  $ZnCo_2O_4$  with crystallite size between 7-37 nm. The densities of sintered oxides was evaluated by different methods are approximately same. The superhydrophilicity of the sintered oxides was investigated by wetting experiments, by the sessile drop technique were carried out at room temperature in air to determine the surface and interfacial interactions.

**Keywords:**  $ZnCo_2O_4$  nanostructure, XRD, TG/DTA, EDX, SEM, TEM.

---

### INTRODUCTION

In recent years Nanocrystalline zinc cobaltite spinal ( $ZnCo_2O_4$ ) [1] have been extensively studied owing to their potential uses in many application such as solar energy cells as photoelectric energy conversion materials [2-3], Photo catalyst [4-5]. The basis and more significant application of ferromagnetic semiconductors have raised tremendous scope for study of these spinals for application such as in spintronics [6]. Among many semiconductors materials  $ZnCo_2O_4$  is one potential materials is solar energy conversion and photo catalytic field die to its photo chemicals properties similar to  $TiO_2$  [7-8]. A large number of metal oxides [9], mixed oxides and Ferrites has shows sensitivity to certain gas species spinal compounds with a

general formula  $AB_2O_4$ , have also been proved as important oxides in gas sensors and have been investigate for the detection of both oxidizing and reducing gases  $NiFe_2O_4$ ,  $MnFe_2O_4$  and  $ZnFe_2O_4$  spinal ferrites have been extensively studied for various oxidizing gas sensing applications [10-11]. We have therefore adopted the combustion synthesis route to obtain nanosized  $ZnCo_2O_4$  suitable for gas sensing application. Semiconductors gas sensors present the property of changing the conductivity of the sensing material when this is exposed to different atmospheric gas. The gas sensing mechanism usually depends on the operating temperature. The optimum working temperature of the semiconductor sensors depends on the gas atmosphere and on the properties of the sensors materials selected in every case [12-13].

Conventional semiconducting oxides can be prepared by a variety of methods such as Czochralski method [14], Conventional solid state methods [15], sol gel route [16], Co-precipitation [17] and the hydrothermal reaction over an extensive period [18]. Recently combustion synthesis [19] has emerged as attractive technique for the synthesis of homogeneous high purity and crystalline oxide powder at significantly lower temperature then the conventional synthesis methods. All these techniques require shorter time periods and using less amounts of external energy [20-21]. Also further it has been observed that, the synthesized powder with combustion process retain their nanocrystalline structure even after sintering which is extremely useful for many device applications [22]. Combustion synthesis technique has been found and developed for number of applications in the chemical and ceramic process [23] compared with the other synthesis method has the different advantages of shorting the reaction time, giving small particle size products with narrow particle size distribution, high-purity and development which make possible to obtain spinal oxides in the form of ultrafine or nanoparticles [24-25].

The present research, analyze the synthesis of an n-type spinal  $ZnCo_2O_4$  by the combustion method with an average crystalline size of 7.12-37.29 nm. The superhydrophilicity of the sintered oxides was investigated by wetting experiments by the sessile drop technique was carried out at room temperature in air to determine the surface and interfacial interactions.

## MATERIALS AND METHODS

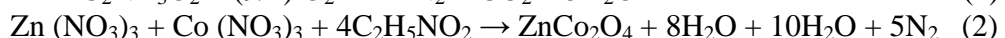
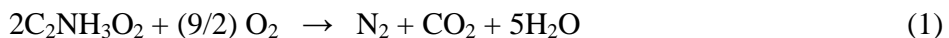
### *Powder preparation*

In present research work synthesized  $ZnCo_2O_4$  powder were prepared using combustion synthesis with different molar composition of fuel subsequently the molar composition was maintained constant and process carried out under varying synthesis temperatures.[26]

Zinc cobalt oxide ( $ZnCo_2O_4$ ) was synthesized using the modified solution combustion technique starting from solution of  $Zn (NO_3)_2 \cdot 6H_2O$  (7.43g),  $(Co (NO_3)_2 \cdot 6H_2O$  (7.27g) and glycine (6.05g). glycine possess ability of high heat of combustion. It is an organic fuel and provides a platform for redox reactions during the course of combustion. Initially the Zinc nitrates, Cobalt nitrates and glycine are taken in the proportion of 1:1:4 in stoichiometric amount and dissolved in a 250 ml beaker to made homogenous paste. Formed paste was evaporated on hot plate in temperature range  $70^0C$  to  $80^0C$  gives thick gel. The gel was kept on a hot plate for auto combustion and heated in the temperature range  $170^0C$  to  $180^0C$ . The nanocrystalline  $ZnCo_2O_4$  powder was formed within 40-50 minute which sintered at about 300, 500, 800 and  $1000^0C$  for about 4 hours then get black color shining powder of  $ZnCo_2O_4$  in nanocrystalline form.

The as -prepared samples were characterized by TG/DTA thermal analyzer (SDT Q600 V 20.9 Build 20), XRD Philips Analytic X-ray B.V. (PW-3710 Based Model diffraction analysis using Cu-K<sub>α</sub> radiation), scanning electron microscope (SEM, JEOL JED 2300) coupled with an energy dispersive spectrometer (EDS JEOL 6360 LA), A JEOL JEM-200 CX transmission electron microscope operating at 200 kV analysis.

## RESULT AND DISCUSSION



TG-DTA analysis was performed at a heating rate of  $10^0 \text{K min}^{-1}$  to investigate the thermal properties of  $\text{ZnCo}_2\text{O}_4$ . The TG spectrum and its 1<sup>st</sup> derivative represented in Figure 1 show the thermal decomposition of  $\text{ZnCo}_2\text{O}_4$ , the curve indicates that the slight weight loss of about 13.2% at temperature up to  $140^0\text{C}$  in  $\text{ZnCo}_2\text{O}_4$  powder due to little loss of moisture, carbon dioxide and nitrogen gas. The DTA curve of  $\text{ZnCo}_2\text{O}_4$  recorded in static air shown in Figure 1 the curve shows that  $\text{ZnCo}_2\text{O}_4$  did not decompose but weight loss was due to dehydrogenation, decarboxylation and denitration. Further weight loss of about 28% between the temperature range  $300^0\text{C}$  to  $400^0\text{C}$  and continuous loss in weight about 48% up to  $600^0\text{C}$  is attributed to loss of organic materials and yield final product at  $650^0\text{C}$ . Weight loss and weight gained was very negligible. These indicating that the synthesized powder was almost remain stable from the beginning. The formed temperature in the present research work was found to be comparatively similar than that reported corresponding solid state reaction route [27].

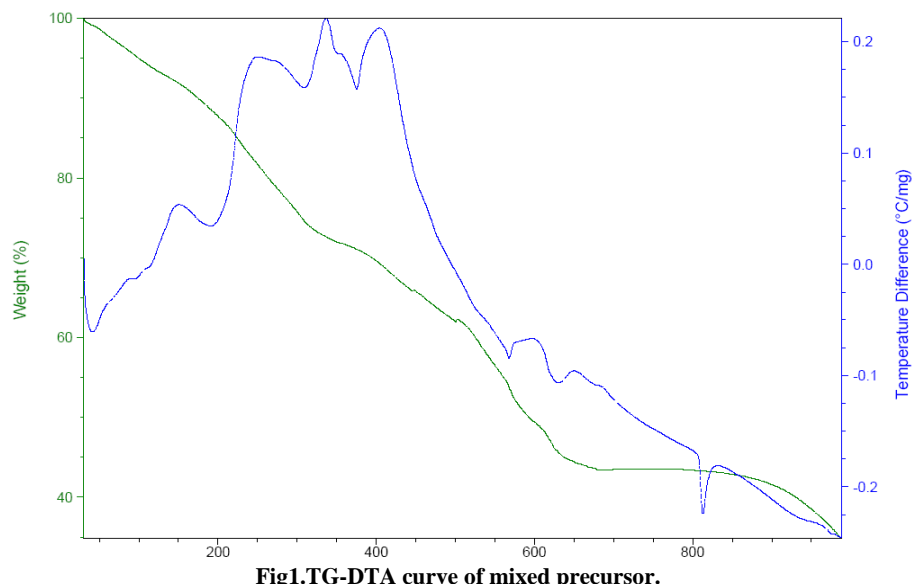


Fig1.TG-DTA curve of mixed precursor.

The X-ray diffraction patterns of each sample were studied at different temperatures and were shown in Figure 2. The observed d values compared with standard d values and was observed in agreement with standard d value i.e. JCPDS data. (Card number 82-1042). The cubic structure possesses the may be attributed to the different preparation method which may yield different structural defects. The crystalline size was determined from full width of half maximum

(FWHM) with the most intense peak obtained which shown scanning of X-ray diffraction pattern. The crystallite size was calculated by using represented Scherer equation [28-29]

$$d = 0.9\lambda / \beta \cos \theta.$$

Where  $d$  is the crystalline size,  $\lambda$  is the X-ray wavelength of the Cu K $\alpha$  source ( $\lambda=1.54056 \text{ \AA}^0$ ),  $\beta$  is the FWHM of the most predominant peak at 100 % intensity,  $\theta$  is the Braggs angle at which peak is recorded. In order to obtain pure nanocrystalline ZnCo<sub>2</sub>O<sub>4</sub> particles and understand the thermal characterizations as prepared ZnCo<sub>2</sub>O<sub>4</sub> powder is further calcinated at 180, 300, 500, 800 and 1000 $^0\text{C}$  respectively (the calcinated temperature assigned as  $T_C$ ). Figure 2 present XRD patterns for ZnCo<sub>2</sub>O<sub>4</sub> oxide nanoparticles. The effects of the calcinations temperature on the crystallite size of ZnCo<sub>2</sub>O<sub>4</sub> particles can be demonstrated. Traces of ZnCo<sub>2</sub>O<sub>4</sub> crystallites phases (111), (220), (311), (222), (400), (311), (422) and (511) are detected in the XRD pattern for all calcinated temperatures and then their intensities increase abruptly when the  $T_C$  above 1000 $^0\text{C}$ . In general, the sharpness of the XRD peak (i.e. high crystallinity) is increased as the  $T_C$  increases. According to the (222) diffraction pattern of ZnCo<sub>2</sub>O<sub>4</sub> crystalline, the particle size of ZnCo<sub>2</sub>O<sub>4</sub> can be calculated from the full width at half-maximum using the Scherrer equation. Obviously, the particle size of ZnCo<sub>2</sub>O<sub>4</sub> changes as the  $T_C$  controlled fewer than 180, 300, 500, 800 and 1000 $^0\text{C}$ , the order is 7, 8, 9, 12 and 37 nm respectively. These indicate that the crystallinity of ZnCo<sub>2</sub>O<sub>4</sub> is accelerated as the  $T_C$  above 500 $^0\text{C}$  illustrates the relationship between the annealing temperature and the average crystal size of the ZnCo<sub>2</sub>O<sub>4</sub> nanoparticles. It is obvious that the ZnCo<sub>2</sub>O<sub>4</sub> nanoparticle grows slowly at range 300-500 $^0\text{C}$  and 800-1000 $^0\text{C}$ , respectively and it was shown that nanoparticle grow rapidly at 800 $^0\text{C}$ .

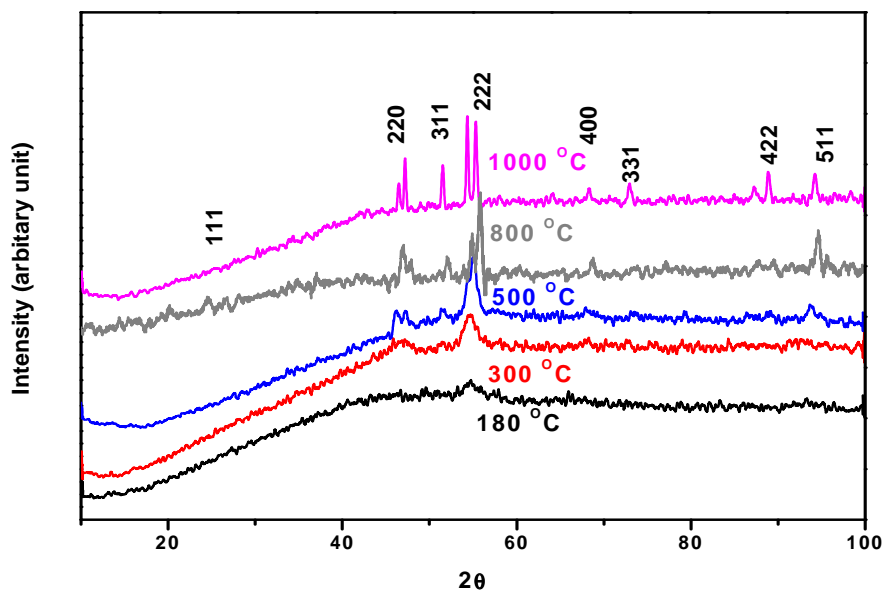
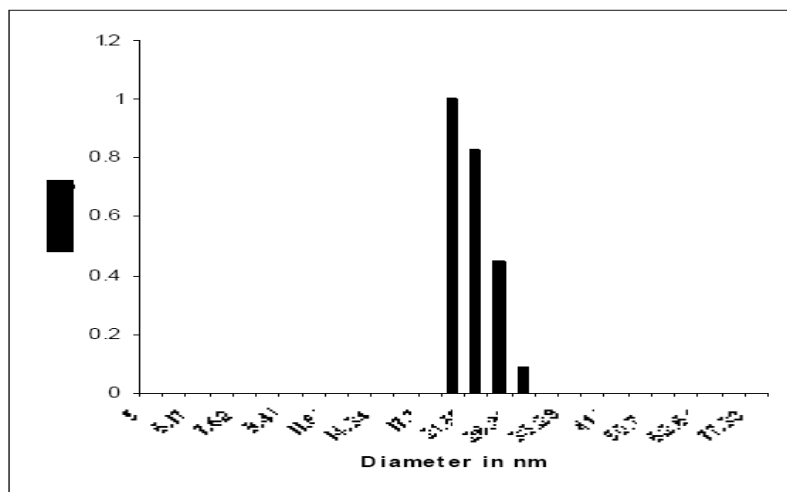


Fig2. XRD patterns of calcinied mixed precursor at 180,300,500,800 and 1000 $^0\text{C}$ .for4h.

Particle size distribution studies. Fig. 3 has been carried out by using dynamic light scattering techniques. (DLS via Laser input energy of 632 nm) It was observed that zinc cobalt oxide nanoparticles have narrow size distribute within the range of about 25-30 nm. Which are well match with calculated value and was calculated it from Debye-Scherrer equation.



**Fig3. Particle size Distribution of as prepared ZnCo<sub>2</sub>O<sub>4</sub> powder**

The microstructure of the 800°C sintered samples can be visualized from scanning electron microscope (SEM) tool. Fig. 4 depicts SEM images of ZnCo<sub>2</sub>O<sub>4</sub> powder it shown the particle morphology of high resolution the particle are most irregular in shape with a nanosize range of 100-200 nm some particles are found as agglomerations containing very fine particles. It can be observed that ZnCo<sub>2</sub>O<sub>4</sub> have uniformed size of about 5μm. It seems that surfaces are smooth, spongy and pores are seen in the micrograph.

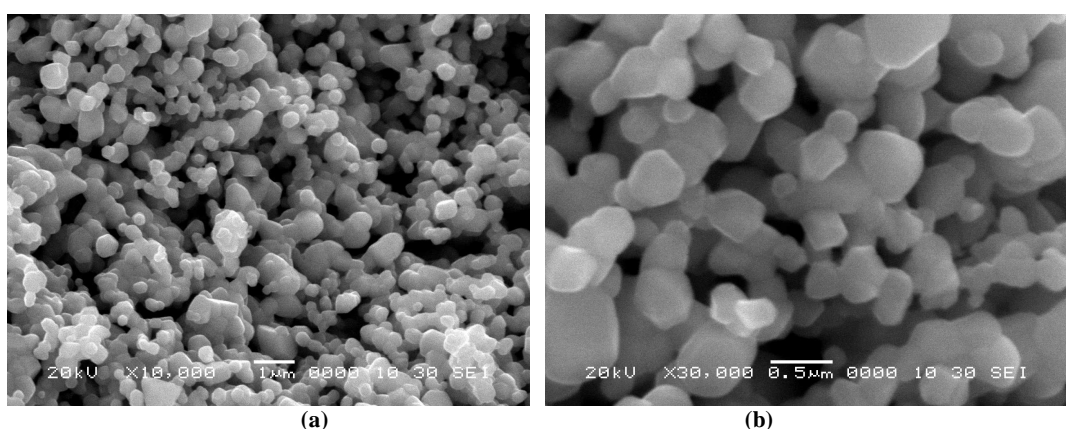


**Fig4. SEM images of the self combustion product the powder annealed at 800°C at (a) low resolution (b) high resolution.**

The energy dispersive X-ray microanalysis was carried out to know the presence of zinc, cobalt and oxygen peaks confirms in Fig. 4

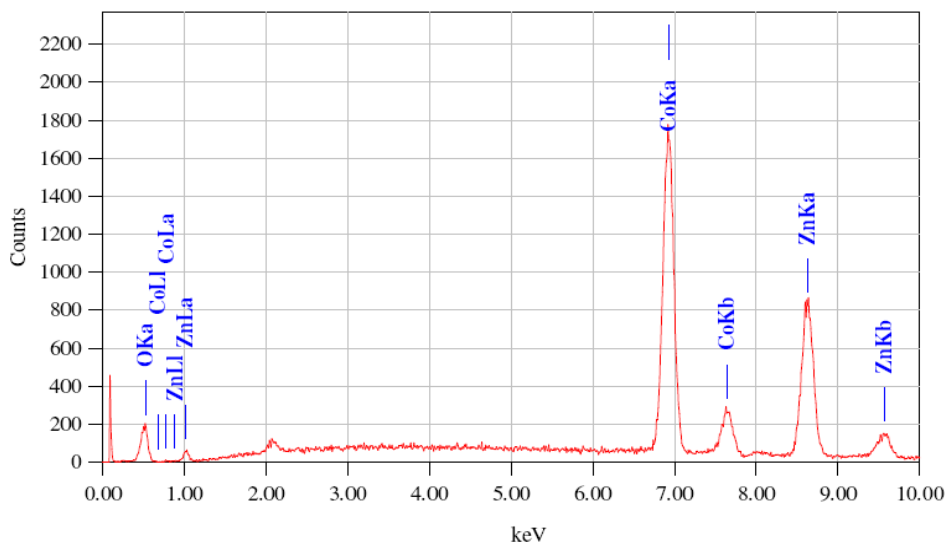
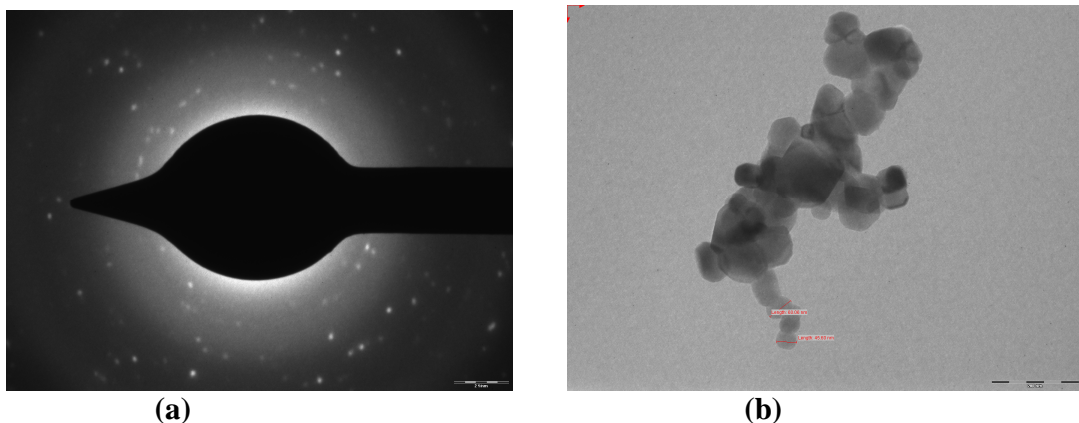


Fig5. EDX pattern of mixed precursor.

The TEM image of the mixed precursor calcined at  $800^{\circ}\text{C}$  for 2h are shown in Fig. 6. It indicates the presence of  $\text{ZnCo}_2\text{O}_4$  nanoparticles with size 30-40 nm which form bead type of oriental aggregation throughout the region. The selected area electron diffraction (SAED) pattern shown in Fig. 6 (a) which shows that spot type pattern is indicates the presence of single crystalline particles. No evidence was found for more than one pattern, suggesting the single phage nature of the material.

Fig.6. TEM (a) images of nanostructured  $\text{ZnCo}_2\text{O}_4$  (b) SAED pattern.

### Density measurement

#### a) Density evaluation from X-ray data

The X-ray density of the samples has been computed from the values of lattice parameters using the formula [30-31]

$$d = 8M/Na^3,$$

Where 8 represent the number of molecules in a unit cell of a spinel lattice, M the molecular weight of the sample, N the Avogadro's number and a is the lattice parameter of sample.

The lattice constant for the cubic was calculated using the equation

$$d = a / (h^2 + k^2 + l^2)^{1/2}.$$

*b) Tap density*

The as prepared  $\text{ZnCo}_2\text{O}_4$  was crushed in an agate mortar using a pestle and mortar. A known amount of this powder was filled into a graduated cylinder of 10 ml capacity. The cylinder was tapped until the powder level remain unchanged. The volume occupy by the powder was noted. The ratio between the weight of the substance and the volume gave tap density [32].

b) *Powder density*

The powder densities were measured using Archimedes principal [33] with a picometer and xylene as a liquid medium. The pyrometer volume of 10 ml was used. The following weight were taken and used for the density calculation.

Weight of the bottle +  $W_{1g}$ ,

Weight of the bottle + substance =  $W_{2g}$ ,

Weight of the bottle + substance =  $W_{2g}$ ,

Weight of the bottle + xylene +  $W_{4g}$ .

### Density of xylene $\equiv S_{\text{el.}}$

$$\rho = (W_2 - W_1) s_{\text{sol}} / (W_4 - W_3) + (W_2 - W_1)$$

Table 1. Densities of  $ZnCo_2O_4$  in  $kg/m^3$

Sample	Density from XRD	Tap density	Bulk density
ZnCO <sub>2</sub> O <sub>4</sub>	4170.22	4188.12	4138.88

## Superhydrophilic Test

Wet ability of pallet shows behavior of water droplet on upper surface of material depends on surface energy and surface roughness of material. Thomas Young had described the force acting on a liquid droplet spreading on surface so-called contact angle ( $\theta$ ) is related to interfacial energies acting between the solid-liquid ( $\gamma_{SL}$ ), solid-vapor ( $\gamma_{SV}$ ) and liquid-vapor ( $\gamma_{LV}$ ) given by following relation.

$$\cos \theta = \frac{(\gamma_{sv} - \gamma_{sl})}{\gamma_{lv}} \quad \dots \dots \dots \quad (3)$$

The expression given by Equation 3 is strictly valid only for surfaces that are atomically smooth, chemically homogeneous and those that don't change their characteristics due to interactions of the probing liquid with the substratum or any other outside force. Wenzel regime liquid wets the surface but the measured contact angle  $\theta^*$  differs from the "true" contact angle  $\theta$  by Wenzel's equation for rough surface  $r > 1$ .

Where  $r$  is the roughness factor of the 9/surface. The wet ability nature of our synthesized material is super hydrophilic in the Wenzel because of highly rough surface nature was clearly seen from SEM images with consideration given to the surface roughness. Fig. 7 (a-b) shows the image of contact angle on rough surface of zinc cobalt oxide material. It was seen that contact angle of material is  $\theta = 0$  hence material in superhydrophilic  $\theta \leq 5$  may be due to high energy surface and their porous nature.

#### **In to characterization**

Wetting experiment of synthesized pure zinc cobalt oxide evaluated by contact angle measurement were performed by the sessile drop method using advanced goniometer apparatus (Model110, Ram hart Instrument Co., USA) and distilled water droplets of 0.01ml were delivered to surface of zinc cobalt oxide pellet material at different points.

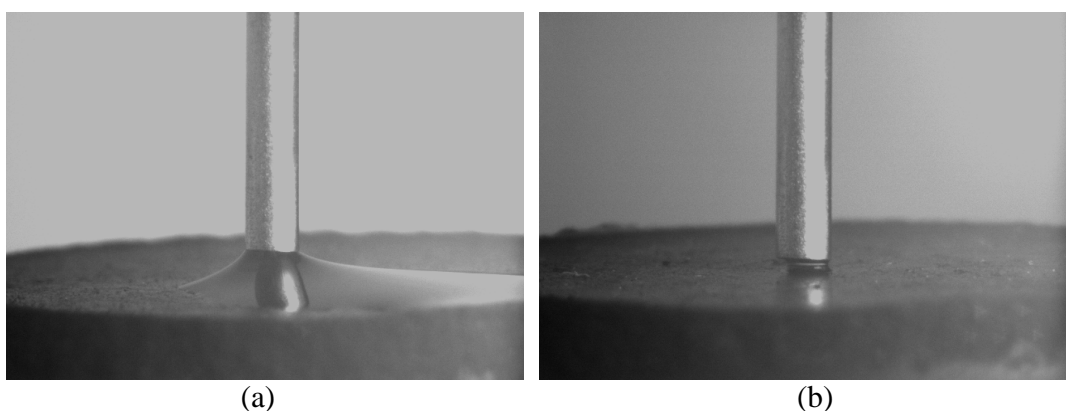


**Fig.7 (a-b) Photograph of measured contact angle on rough surface of zinc cobalt oxide (pellet) material.**

#### **CONCLUSION**

Nanocrystalline  $ZnCo_2O_4$  has been successfully synthesized by self combustion route. TG-DTA analysis indicates the phase formation was carried out at  $650^0C$ . The route may be used for the synthesis of other metal oxide. XRD technique was shown the average crystal size of the  $ZnCo_2O_4$  nanoparticles ranges from about 7-37 nm at  $180-1000^0C$  respectively. Elemental analysis confirmed by using EDX. SEM micrographs show the material is porous in nature. TEM image shows grain size of the material was 30 nm. Density was carried out by different technique and it was found to approximately same. Wetability of this material obtained from contact angle goniometer. The contact angle  $\theta$  was zero, which indicates that oxide material was superhydrophilic in nature.

#### **REFERENCES**

- [1] M. M. Abou-Sekkina, Khaled M. Elsabawy and F. G. Elmetwaly *Advances in Applied Science Research*, **2010**, 1 (1): 34-43
- [2] Y. Muyata, S. Fukuta, S. Ishikawa, S. Yakayama, Si. *Energy Mater Sol. Cell* **2000**, 62, 157.
- [3] Y. Gian , X. Zhang , Y. Bai , T. Li , X. Tang , E. Wang , S. Dang , *J. of Nanopartical Res.* **(2000)** , 2 ,191.
- [4] W. Piekarczyk, P. Oeshev, and A. Toshev. *Mat. Res. Bull.* **1988**, 23, 1299.

[5] T. L. Marta, *Appl. Catal. B* **1989-90**, 23, 420.

[6] S. J. Pearton , C. R. Abmathy , A.F. Herbrd , L. A. Baather *J. Appl. Phys.* **2003** 1, 23.

[7] Y. Hao, M. Yang L. Zhang, S. Cai. *Sol. Energy Mater, Sol. Cells* **2000**, 60, 349.

[8] D.Y.Goswami, S.Vijayaraghavan, S. Lu, G. Tamm, *Sol. Eng. B* **2004**, 108, 2.

[9] Amrut. S. Lanje, Satish J. Sharma, Ramchandara B. Pode, Raghuman S.Ningthoujam *Advances in Applied Science Research*, **2010**, 1 (2): 36-40

[10] Y. Shimizu, S. Kusano, H. Kuwayama, K. Tanaka, M. Eqashira, *J. Am. Ceram. Soc.* **1990** , 73, 818-824.

[11] C. Gopal Raddy, S. Manorama , V. Rao, *J. Mater. Sci. Lett.* **2000**, 19, 775-778.

[12] A. Phani, S. Manorma, V. Rao, , *Appl. Phys. Lett.* **1995**, 66, 3489-3491

[13] V. Ramaswamy, R.M. Vimalathithan1 and V. Ponnusamy, *Advances in Applied Science Research*, **2010**: 1 (3), 197-204

[14] R. Graser, E. Pitt, A. Scharmann, G. Zimmerer *Phys. Status Solid B*, **1975**,359

[15] K. Krezhov and P. Konstantinav *J. Phys. Condens. Matters*, **1993** 9287

[16] X. Wei, D. Chen, W. Tang, *Mater.Chem.Phys.* **2007**, 103, 54–58.

[17] S. Christoskoe, M. Stojanova, M. Gerogieva, D. Mehandzhiev, , *Thermochim. Acta* **1997**,292, 77–83.

[18] S. Deka and P. Joy *Chem mater. Conn.* **2000** ,9, 3-5.

[19] N. Kasapoglu, A. Baykal, Y.Koseoglu, M.S.Topark.. *Mater.* **2007**, 57 (5), 441-444.

[20] C. Kital, Introduction to solid state physics 7<sup>th</sup> ed John Willey and Son Singapore **2000** P. 449.

[21] T. Ohgushi, K. Ishimaru, *J. Am. Ceram. Soc.* **2001**, 84, 321.

[22] C. Jansen, A. Arafat and H. Robson [eds] synthesis if microporous materials Vol 1 Van. Nostrand Reinhold, New York **1992**, p 507.

[23] K. Petrov L. Markov, R. Locheva, P. Rachev *J. Mater. Sci.* **1988** 23,181.

[24] S. R. Bamane and A. M. Chavan, Ph.D.Thesis **1996** p175 Shivaji University Kolhapur (MS) India.

[25] S. Bhaduri, S. B. Bradbury, microstrutural and mechanical properties of nanocrystalline spinal and releted composite Ceram. Int. **2002**, 28, 153.

[26] Sanjay M. Khetre, H.V.Jadhav, S.V.Bangale, P.N.Jagdale, S.R.Bamane *Advances in Applied Science Research*, **2011**, 2, (2) 252-259.

[27] K. Omata, T. Takada, S. Kasahara, *J.Appl. Catal.A:Gen.* **1996** 146, 255-267.

[28] Ashish Tiwaria, S A Khan, R S Kher, *Advances in Applied Science Research*, **2011**: 2 (1),105.

[29] S. Srikanth, N. Suriyanarayanan, S. Prabahar, V. Balasubramanian, D. Kathirvel, *Advances in Applied Science Research*, **2011**: 2 (1) , 95.

[30] J. Smith, H.P. Wijn, N.N. Phillips and Gloeilampenjabricken Eindhoven Ferrites (Holland **1959** ,144A.

[31] A. Venkataraman A.V. Hiremath, K.S. Date and M.S. Kulkarni *Bull. Mater.Sci.* **2000**, 24,101.

[32] S. Kinsman, T.H.Richardson, and R.V. Peterson (New York: Academic Press) Systematic materials analysis Vol. 4 p.200.

[33] P.H. Klug and L. Alexander X-ray diffraction procedure (New-York: John Wily) (**1962**).